

https://doi.org/10.1070/QEL17551

Enhancing the time contrast and power of femtosecond laser pulses by an optical wedge with cubic nonlinearity

E.A. Khazanov

Abstract. **A method is proposed for enhancing the time-domain contrast of femtosecond laser pulses under nonlinear pulse compression by means of spectrum broadening due to the self-phase modulation with a following reflection from chirped mirrors. The contrast increases because the radiation of the pedestal is blocked by a square screen arranged in a focal plane of a unit-magnification telescope, and the main pulse 'bypasses' the screen, because a wedge in front of the telescope declines the pulse to a large angle due to a cubic nonlinearity.**

Keywords: *time-domain contrast, ultrahigh-power laser, cubic nonlinearity.*

1. Introduction

Many experiments on studying matter properties in extreme conditions require both a large peak power of a laser pulse, and a high time-domain contrast. In recent years, the method of nonlinear compression is actively developed for increasing the power, in which a plane-parallel plate introducing a phase modulation and chirped mirrors introducing a negative dispersion are employed. The method is called thin film compression (TFC) [1], compression after compressor approach (CafCA) [2], or post-compression [3]. Multiple shortening of femtosecond laser pulses actually with no energy losses was demonstrated for pulse energies of several [4, 5] or even dozens of joules [6, 7] (see review [8]).

Under the time-domain contrast is meant the ratio of the pulse maximum intensity to the intensity at pulse wings. In many experiments, a high value of the far time contrast (1–1000 ps from the peak of the main pulse) is rather important because if this value is low, the target breaks prior to arrival of the main pulse. A far contrast is determined by a value of the pulse pedestal, which usually arises from an amplified spontaneous emission in laser amplifiers comprised in a CPA laser (chirped pulse amplification) [9] or due to amplified parametric emission in OPCPA lasers (optical parametrical chirped pulse amplification) [10]. The contrast can be increased by using plasma mirrors [11], second-harmonic generation [12], and nonlinear optical methods based (as in the present work) on cubic nonlinearity with the employment of cross-polarised wave polarisation [13], spectrum broadening under self-phase modulation [14, 15], and nonlinear Mach–Zehnder interferometer [16]. In the most of applications, the contrast in the focal plane of an optical system (on a target) is important rather than in the near field of radiation.

In the present work, a method for increasing the time-domain contrast on a target is proposed based on the employment of an optical wedge in a laser beam. The idea is that, according to laws of linear optics, a wave vector of pedestal radiation is declined by a wedge, whereas the wave vector of the main pulse is declined to a different angle because the wedge refraction index n depends on intensity I: $n = n_0 + n_2 I$, where n_2 is the nonlinear refractive index. Hence, the beams of the main pulse and of pedestal are separated in the focal plane by a certain distance. If the distance is sufficiently large, the contrast will substantially increase. By using the Snell law $\sin\alpha = n\sin\beta$ one can easily show that a wedge with an angle $\delta \ll 1$ declines the radiation wave vector by the angle

$$\Theta_{\rm w} = \delta\left(n\frac{\cos\beta}{\cos\alpha} - 1\right), \tag{1}$$

where α and β are the incident and refraction angles on the first plane of the wedge. From (1), for the change in angle $\Theta_{\rm w}$ due to the nonlinear addition to the refraction index $\Delta n = n_2 I_0$, we find

$$\Theta_{\rm B} = \frac{{\rm d}\Theta_{\rm w}}{{\rm d}n}\Delta n = \delta\frac{n_2 I_0}{\cos\alpha\cos\beta} \tag{2}$$

i.e. the angle between the wave vectors of the pedestal and the main pulse at the instant of maximal pulse intensity (I_0 is the intensity inside the wedge at the pulse maximum). The most interesting is not the absolute value of $\Theta_{\rm B}$, but its value normalised to the diffraction angle $\Theta_{\rm dif}$. For estimate, we may consider a beam (typical for high-power lasers) of diameter $2w$ with a super-Gaussian intensity profile $\exp(-r^{2m}/w^{2m})$. At $m = 3–5$, such a beam has the divergence about 1.5 times greater than a Gaussian beam: $\Theta_{\rm dif} \approx 1.5/(kw)$, where k is the wave vector. Now, from (2) we obtain

$$\Theta_{\rm B}/\Theta_{\rm dif} = B_0/3, \tag{3}$$

where $B_0 = kL_{\max}n_2 I_0$ is the maximal value of the B-integral (nonlinear phase); $L_{\max} = L_0/\cos\beta$ is the maximal light path length in the wedge; L_0 is the wedge thickness for the ray near the wedge base (for simplicity, the thickness of the wedge edge is taken zero). Thus, at a fixed B_0, the ratio $\Theta_{\rm B}/\Theta_{\rm dif}$ depends on neither the incident angle α (for example, a Brewster angle

E.A. Khazanov Institute of Applied Physics, Russian Academy of Sciences, ul. Ulyanova 46, 603950 Nizhny Novgorod, Russia; e-mail: efimkhazanov@gmail.com

Received 8 March 2021
Kvantovaya Elektronika **51** (5) 433–436 (2021)
Translated by N.A. Raspopov

can be used) nor the wedge vertex angle δ and linear refraction index n_0. Due to the effect of beam self-filtration while it propagates in a free space [8, 17], the radiation pulses with the intensity of 10^{12} TW cm^{-2} and more may escape a small-scale self-focusing at very large B values up to 20–25 [18]. Thus, the condition $\Theta_B \gg \Theta_{dif}$ can be fulfilled in practice.

Nevertheless, 'direct' employment of a wedge is actually impossible because of the chromatic aberrations leading to an angular chirp. Estimates show that the angle $\Theta_{chrom} = (d\Theta_w/d\omega) \times \Delta\omega$ (where ω is the frequency and $\Delta\omega$ is the FWHM width of the emission spectrum) for pulses of duration 30 fs and shorter is comparable to or even greater than the angle Θ_B. Chromatic aberrations can be substantially suppressed by using an achromatic doublet comprised of oppositely oriented wedges W_I and W_{II} (Fig. 1a) fabricated from different materials with different angles δ_I and δ_{II} and with equal (by the absolute values) chromatic aberrations: $\Theta_{chrom\,I} = \Theta_{chrom\,II}$. Taking into account the opposite orientations of the wedges, this condition provides a zero angular chirp within an accuracy of the next infinitesimal order $(d^2\Theta_w/d\omega^2)$. For the achromatic doublet of wedges W_I and W_{II}, the total angle Θ_B will be equal to the difference of the corresponding angles for each wedge: $\Theta_B = \Theta_{B\,I} - \Theta_{B\,II}$ (the difference rather than the sum, because the wedge vertices are oppositely oriented). The angle for each wedge is determined by formula (2); in the general case, all values in the right side of (2), namely, δ, α, β, n_2, and I_0, differ for these wedges (intensities I_0 differ because of the different incident angles). The only condition imposed on these parameters is the equality of chromatic aberrations $\Theta_{chrom\,I} = \Theta_{chrom\,II}$. In view of these condition, for $\Theta_B = \Theta_{B\,I} - \Theta_{B\,II}$ we obtain, instead of (3), the formula

$$\frac{Q_B}{Q_{dif}} = \frac{B_0}{3}(1 - NDG), \tag{4}$$

where

$$N = \frac{n_{2\,II}}{n_{2\,I}};\; D = \frac{K_I}{K_{II}};\; G = \frac{\cos\alpha_{II}/\cos\beta_{II}}{\cos\alpha_I/\cos\beta_I};$$

and K is the group velocity dispersion. Here, similarly to the above consideration, B_0 is the maximal value of the B-integral, that is, its value for the beam at the base of wedge W_I. By choosing the parameters of wedges W_I and W_{II} such that $NDG \ll 1$ [that is, expression (3) actually does not change], we obtain the wedge without chromatic aberrations, which, however, separates the main pulse from the pedestal with the efficiency actually similar to that of a conventional wedge. If

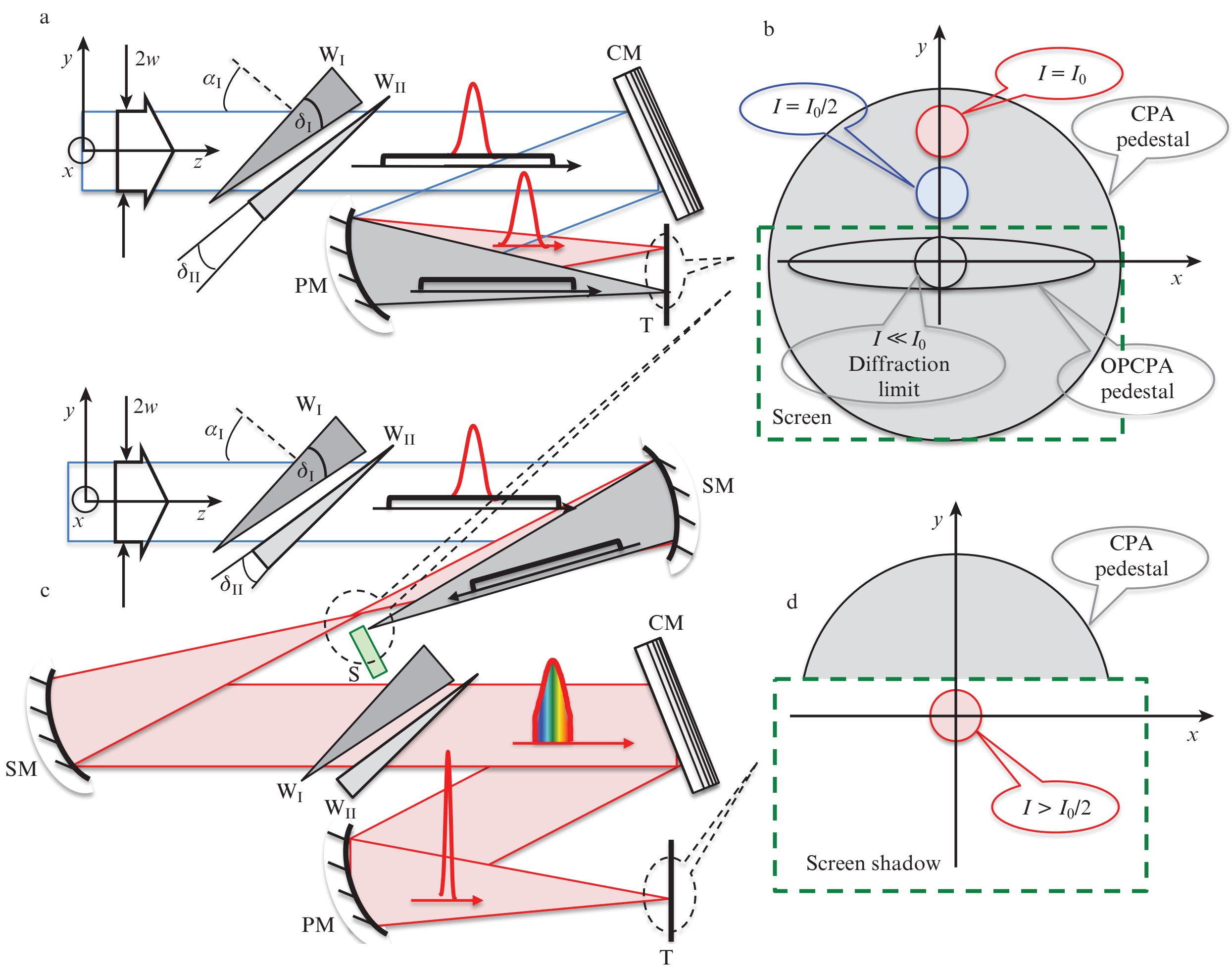

Figure 1. (Colour online) Schematic with one (a) and two (c) achromatic wedges and beam positions at the focal point after the first (b) and second (d) achromatic wedges:
(W_I, W_{II}) wedges forming the achromatic wedge; (SM) spherical mirrors of a telescope; (CM) chirped mirror; (S) rectangular screen, which blocks a low-intensity radiation; (PM) mirror or parabola, focusing the radiation to a target; (T) target.

both the wedges are arranged at equal angles $\alpha_{\rm I} = \alpha_{\rm II}$, then $G \approx 1$. However, if wedge $W_{\rm I}$ is placed at normal incidence, that is, $\alpha_{\rm I} = 0$ and wedge $W_{\rm II}$ is placed at the Brewster angle, then we obtain $G = 1/n_{0\,\rm II} < 1$; at a greater angle $\alpha_{\rm II}$, G will be even less. If wedge materials are the same, then N may become less than unity if crystals with different orientations are used, including cubic crystals. For example, for BaF_2 we have $N = 0.55$ for orientations [001] and [110]. Thus, even in the case of the same material ($D = 1$) it is possible to obtain $NG \ll 1$: for BaF_2 at $\alpha_{\rm II} = 75°$ we have $NG = 0.19$. The efficiency may be greater if wedges $W_{\rm I}$ and $W_{\rm II}$ are fabricated from different materials. For wedge $W_{\rm I}$, a KDP crystal (an ordinary wave) is suitable, which possesses a low dispersion and high nonlinearity. Wedge $W_{\rm II}$ may be fabricated, for example, from $CaCO_3$ (ordinary wave). One more example is a pair of glasses K8 and TPh12. We have $ND = 0.12$ and 0.13 for KDP-$CaCO_3$ at a wavelength of 910 nm and K8-TPf12 at a wavelength of 800 nm, respectively. Hence, an achromatic wedge increases the contrast in a focal plane if

$$B_0/3 \gg \Theta_{\rm noise}/\Theta_{\rm dif}, \tag{5}$$

where $\Theta_{\rm noise}$ is the divergence of pedestal radiation. Figure 1b presents beam dispositions in the focal plane for $B_0 \approx 15$, that is, $\Theta_{\rm B} \approx 5\Theta_{\rm dif}$. In Fig. 1b, the z axis passes through the centre of coordinates. Radiation propagates along this axis according to laws of linear optics (that is, $\Theta_{\rm B} = 0$); hence, the pedestal centre is always at the centre of coordinates. Condition (5) can be easily fulfilled if $\Theta_{\rm noise} \approx \Theta_{\rm dif}$, which is possible for OPCPA lasers in the critical plane of parametrical interaction [19] (the pedestal is shown as an oval), and for OPCPA and CPA lasers with a spatial filter (the pedestal is shown as a small circle). However, the most of CPA-lasers have the pedestal divergence substantially greater than $\Theta_{\rm dif}$ (the pedestal is shown as a large circle) and condition (5) cannot be fulfilled. One more drawback of the method for increasing a contrast shown in Fig. 1a is inevitable inhomogeneity of the B-integral in the beam transverse cross section (along the y coordinate), which is a fee for the contrast increase, because the phase inhomogeneity along the y axis allows a high-power radiation to deviate from the pedestal. Thus, the employment of a wedge (even achromatic one) substantially worsens the compression efficiency as compared to a plane-parallel plate.

These two drawbacks can be eliminated by adding, according to Fig. 1c, a unit-magnification telescope and the second achromatic edge identical to the first one, and by placing a screen in the telescope focal plane (shown in Fig. 1b as a dashed rectangular) for occluding a low-intensity radiation propagating according to linear optics laws. The second achromatic wedge will 'cancel out' the deviation introduced by the first wedge and will 'return' the main pulse in the target plane to the place where the pedestal would be focused if there was not the screen (Fig. 1d). Importantly, in this case the divergence of pedestal radiation $\Theta_{\rm noise}$ may be arbitrary large, because the place of main pulse focusing on the target will be shadowed by the screen (regardless of the value $\Theta_{\rm noise}$). In addition, the total B-integral accumulated in both the achromatic wedges will be uniform along both x and y coordinates of the beam because two wedge pairs totally act as two plane-parallel plates. It is an important advantage as compared to the much simpler variant shown in Fig. 1a because the pulse compression by chirped mirrors will be as efficient as under self-phase modulation in a plane-parallel plate.

The compression will be imperfect, because the leading and trailing edges of the main pulse are blocked by the screen due their moderate intensity. Nevertheless, the main part of the pulse with a wide spectrum and linear chirp will 'bypass' the screen, which will provide a multiple compression at a large B_0. Note that achromatic wedges can be placed inside the telescope: one wedge in the converging beam and the other in the diverging. In this case, wedges $W_{\rm I}$ and $W_{\rm II}$ may be arranged at a certain distance from each other, which will make the radiation intensities in the wedges different and the choice of materials for wedges will be simpler.

Thus, the arrangement of an achromatic wedge in front of the focusing parabola makes it possible to increase the contrast of a laser pulse in the focus under the condition that at least along one coordinate the divergence of pedestal radiation is close to a diffraction limit, which is characteristic of OPCPA lasers (Figs 1a and 1b). If two achromatic wedges are used, between which a unit-magnification telescope is placed with a rectangular screen in the focal plane and chirped mirrors (Figs 1c and 1d), then the contrast substantially increases at arbitrary divergence of the pedestal radiation, and the peak power increases due to the nonlinear compression. Accurate values of the increase in the contrast and pulse power and wedge optimal materials and parameters can be found from thorough numerical simulations. Results of such simulations will be presented in a separate publication.

Acknowledgements. The work was supported by the Centre of Excellence "Center of Photonics" funded by the Ministry of Science and High Education of the Russian Federation (Agreement No. 075-15-2020-906).

References

1. Mourou G., Mironov S., Khazanov E., Sergeev A. *Europ. Phys. J. Spec. Top.*, **223**, 1181 (2014).
2. Ginzburg V.N., Yakovlev I.V., Zuev A.S., Korobeinikova A.P., Kochetkov A.A., Kuz'min A.A., Mironov S.Yu., Shaikin A.A., Shaikin I.A., Khazanov E.A. *Quantum Electron.*, **49**, 299 (2019) [*Kvantovaya Elektron.*, **49**, 299 (2019)].
3. Balla P., Bin Wahid A., Sytcevich I., Guo C., Viotti A.-L., Silletti L., Cartella A., Alisauskas S., Tavakol H., Grosse-Wortmann U., Schönberg A., Seidel M., Trabattoni A., Manschwetus B., Lang T., Calegari F., Couairon A., L'Huillier A., Arnold C.L., Hartl I., Heyl C.M. *Opt. Lett.*, **45**, 2572 (2020).
4. Chvykov V., Radier C., Chriaux G., Kalinchenko G., Yanovsky V., Mourou G., in *Proc. Conference on Lasers and Electro-Optics 2010* (California, San Jose: Optical Society of America, 2010).
5. Mironov S.Y., Fourmaux S., Lassonde P., Ginzburg V.N., Payeur S., Kieffer J.C., Khazanov E.A., Mourou G. *Appl. Phys. Lett.*, **116**, 241101 (2020).
6. Ginzburg V., Yakovlev I., Zuev A., Korobeynikova A., Kochetkov A., Kuzmin A., Mironov S., Shaykin A., Shaikin I., Khazanov E., Mourou G. *Phys. Rev. A*, **101**, 013829 (2020).
7. Ginzburg V.N., Yakovlev I.V., Zuev A.S., Korobeinikova A.P., Kochetkov A.A., Kuz'min A.A., Mironov S.Yu., Shaikin A.A., Shaikin I.A., Khazanov E.A. *Quantum Electron.*, **50**, 331 (2020) [*Kvantovaya Elektron.*, **50**, 331 (2020)].
8. Khazanov E.A., Mironov S.Yu., Mourou G. *Phys. Usp.*, **62**, 1096 (2019) [*Usp. Fiz. Nauk*, **189**, 1173 (2019)].
9. Strickland D., Mourou G. *Opt. Commun.*, **56**, 219 (1985).
10. Dubietis A., Jonusauskas G., Piskarskas A. *Opt. Commun.*, **88**, 437 (1992).
11. Levy A., Ceccotti T., D'Oliveira P., Réau F., Perdrix M., Quéré F., Monot P., Bougeard M., Lagadec H., Martin P., Geindre J.-P., Audebert P. *Opt. Lett.*, **32**, 310 (2007).
12. Mironov S.Y., Lozhkarev V.V., Ginzburg V.N., Khazanov E.A. *Appl. Opt.*, **48**, 2051 (2009).

13. Jullien A., Albert O., Burgy F., Hamoniaux G., Rousseau J.-P., Chambaret J.-P., Augé-Rochereau F., Chériaux G., Etchepare J., Minkovski N., Saltiel S.M. *Opt. Lett*, **30**, 920 (2005).
14. Buldt J., Müller M., Klas R., Eidam T., Limpert J., Tünnermann A. *Opt. Lett*, **42**, 3761 (2017).
15. Mironov S., Starodubtsev M., Khazanov E. *Opt. Lett.*, **46**, 1620 (2021).
16. Khazanov E.A., Mironov S.Yu. *Quantum Electron.*, **49**, 337 (2019) [*Kvantovaya Elektron.*, **49**, 337 (2019)].
17. Mironov S.Y., Lozhkarev V.V., Ginzburg V.N., Yakovlev I.V., Luchinin G., Shaykin A.A., Khazanov E.A., Babin A.A., Novikov E., Fadeev S., Sergeev A.M., Mourou G.A. *J. Sel. Top. Quantum Electron.*, **18**, 7 (2010).
18. Mironov S., Lozhkarev V., Luchinin G., Shaykin A., Khazanov E. *Appl. Phys. B: Lasers Opt.*, **113**, 147 (2013).
19. Lozhkarev V.V., Freidman G.I., Ginzburg V.N., Khazanov E.A., Palashov O.V., Sergeev A.M., Yakovlev I.V. *Laser Phys.*, **15**, 1319 (2005).